FLUORESCENCE SPECTROSCOPIC AND KINETIC STUDY OF TRIETHYLAMINE EXCIPLEX FORMATION WITH ETHANOL

GOTTFRIED KÖHLER

Institute for Theoretical Chemistry and Radiation Chemistry, University of Vienna, Währingerstrasse 38, 1090 Vienna (Austria)

(Received March 17, 1986; in revised form April 23, 1986)

Summary

Exciplex formation of triethylamine with ethanol and with deuterated ethanol at low alcohol concentrations in hydrocarbon solutions is shown by steady state and time-resolved fluorescence spectroscopy. The observed spectra and the decay kinetics show the appearance of three exciplex structures which can be discriminated by temperature and deuterium isotope effects. The spectrum of the primarily formed 1:1 heterodimer overlaps significantly with the monomer spectrum (spectral shift is 800 cm^{-1}) and equivalent associations are found with tetrahydrofuran. The photophysical parameters change only slightly on complexation. Two further exciplex emissions with large spectral shifts compared with the monomer (4500 cm^{-1} and 9000 cm^{-1}) arise at ethanol concentrations above 0.02 M, together with a diminution of the quantum yield. Complexation with non-deuterated ethanol leads primarily to high energy emissive structures and equilibrium is attained, as they decay with a common lifetime. Deuteration of ethanol results in a stabilization of the lowest energy exciplex, which is populated irreversibly. Exciplex structures are discussed, with reference to *ab initio* model calculations.

1. Introduction

The phenomenon of complex formation in the electronically excited state to give either excimers or exciplexes is widely found in the emission of aromatic molecules in the condensed phase and has received considerable attention [1, 2]. The mechanisms leading to their formation and properties have been studied in detail.

Information on the production of excited complexes of saturated closed shell compounds is only scarce in comparison with that available for aromatic molecules. This stems essentially from the fact that excitation of saturated compounds rarely results in an intense fluorescence. Tertiary

0047-2670/86/$3.50

amines, such as triethylamine (TEA) or quinuclidine (ABCO), are the most prominent exceptions as they show fluorescence with high quantum yields in the gas phase [3] as well as in hydrocarbon solutions [4, 5].

Saturated amines are well-known electron donors, and emission from charge transfer complexes with aromatics has been reported [6]. In these cases, however, excitation was primarily located on the aromatic moiety.

Excitation of tertiary amines leads to Rydberg-type excited states characterized by an excited orbital of large spatial extension [7, 8]. Such states are assumed to undergo strong perturbations resulting from interactions with the surrounding molecules, and this is demonstrated by efficient fluorescence quenching in polar solvents [5, 9]. The only polar solvent media in which fluorescence from these compounds is found are saturated ethers, for example diethyl ether or tetrahydrofuran (THF) [10]. The emission spectra in such solvents shift considerably to lower energies. No evidence for the formation of solute–solvent exciplexes was found.

In more polar solvents such as alcohols or water, emission from these compounds is no longer observed and in water-saturated hydrocarbons some broadening of the emission compared with pure hydrocarbons was reported [5, 9]. For various other organic compounds (*e.g.* acetonitrile, acetic acid and halogenated hydrocarbons) efficient fluorescence quenching of the amine fluorescence has been described recently [11]. However, exciplex emission was not found for the studied quenchers and the mechanisms were discussed in terms of energy and charge transfer [11].

In contrast, strong excimer emission was described in detail for the cage amines ABCO and 1-azaadamantane in *n*-hexane solution [12, 13]. These excimers are characterized by broad very red-shifted bands ($\nu^{max} \approx 26\,600$ cm^{-1}), and binding energies of 48 kJ mol^{-1} were obtained. Other amines exclusively show self-quenching in solution [14].

We have recently reported some preliminary observations on 1:1 exciplex formation in the TEA–ethanol system in *n*-hexane solution [15]. Shifts of the spectra resulting from complexation are found to be small and they overlap efficiently with the monomer emission. Association is nearly diffusion controlled. However, indications were found for the formation of various exciplexes with different structures.

In this paper, exciplex formation of TEA with ethanol is studied in detail, and the effects of substrate concentration, deuteration of the alcohol and temperature are reported. This work was undertaken to obtain information on the structures and interactions that characterize the exciplexes of saturated molecules. The results are compared with *ab initio* model calculations on excited ammonia–water complexes performed previously in order to support assignments of exciplex spectra [16]. The work was partly initiated by earlier studies on the excitation-energy dependence of the fluorescence quantum yield of anilines [17, 18] and indoles [19, 20], in which evidence was found for the involvement of Rydberg excited states. It was expected that the results of such a study would lead to a deeper understanding of intermolecular interactions in Rydberg excited states.

2. Experimental details

TEA (pro Analysi, Merck, Darmstadt) was distilled over $LiAlH_4$. *n*-Hexane (for fluorescence spectroscopy, Uvasol, Merck, Darmstadt) was dried by column chromatography over silica gel (Woelm, activity 1) and Al_2O_3 (Aluminia Woelm B, Akt. I) under an argon atmosphere and was stored over 4 Å molecular sieves. Ethanol (Uvasol, Merck, Darmstadt) was purified by distillation and refluxing over molecular 10 Å sieves and THF was purified by distillation prior to use. All the compounds were kept free of moisture during storage. Oxygen was removed by bubbling argon through the pure compounds and the quencher was then added under an argon atmosphere. Removal of oxygen by carrying out freeze–pump–thaw cycles changed the ethanol concentration significantly and thus proved to introduce large errors.

The data from the fluorescence unit, which has been described previously (optics from Zeiss, F.R.G., monochromators M 4 QIII) [21] are read directly by an Apple II microcomputer. The spectra were corrected according to the procedures given in ref. 21 and numerically integrated to obtain absolute quantum yields and the centres of gravity $\langle\tilde{\nu}_f\rangle$ of the spectra defined by

$$\langle\tilde{\nu}_f\rangle = \frac{\int f(\tilde{\nu})\tilde{\nu}\,\mathrm{d}\tilde{\nu}}{\int f(\tilde{\nu})\,\mathrm{d}\tilde{\nu}} \tag{1}$$

$f(\tilde{\nu})$ is the spectral distribution of the fluorescence light given in quanta cm^{-1}. The half-bandwidth (HBW) and the maximum $\tilde{\nu}^{max}$ of the emission were determined automatically from the corrected fluorescence spectra.

Energy-resolved fluorescence decay profiles were measured by time-correlated single-photon counting (Model SP 70, Applied Photophysics Ltd., London, slightly modified in our laboratory). The flash lamp was filled with D_2 gas slightly below atmospheric pressure and run at 45 kHz. At least 10^4 counts were collected in the channel of maximum counts and each decay function was routinely measured with a number of time resolutions.

Decay parameters were obtained by a semilinear multi-exponential least-squares deconvolution program, on the CDC-cyber 720 of the university computer centre, based on a sum-of-exponentials least-squares fit algorithm by Kirkegaard [22]. Plots of weighted residuals, the values of the reduced χ^2, the mean errors and the correlation matrix of the parameters were used to judge the quality of the fits [23]. The fits included all times from the rise of the pulse over at least three decades of counts. The wavelength dependence of the instrumental response function (Philips XP 2020 Q photomultiplier tube; high voltage 2650 V) was measured by various standard compounds (2,5-diphenyloxazole, 2,5-diphenyl-1,3,4-oxadiazole, binaphthyl and 1-tyrosine [24]) and appropriate mixtures, and the origin shift correction was found to be sufficient within the error limits for emission wavelengths below 420 nm [23].

3. Results

3.1. Absorption measurements

The far UV absorption of TEA in *n*-hexane increases gradually below 265 nm ($\epsilon_{245} = 112\ M^{-1}\ cm^{-1}$), it peaks at 210 nm and is structureless. On adding ethanol the absorbance above 230 nm decreases uniformly and the optical density drops by 7.5% and 11% for $c_A = 0.05$ M and $c_A = 0.1$ M ethanol respectively (c_A denotes the formal, *i.e.* added, ethanol concentration) compared with the value in pure *n*-hexane (in ethanol solutions $\epsilon_{245} = 8.5\ M^{-1}\ cm^{-1}$). As most of the residual absorption in pure alcohol can be largely attributed to amine molecules not engaged in hydrogen bonding [25], the fraction of 245 nm light absorbed by TEA–ethanol complexes for $c_A = 0.1$ M should be considerably lower than 0.5%, and thus should not interfere in measurements below this concentration.

3.2. Triethylamine in n-hexane

The corrected fluorescence spectra (normalized to equal height) of TEA in pure *n*-hexane and for the TEA–ethanol and TEA–ethanol-d_1 systems are shown for various alcohol concentrations in Fig. 1. In the pure hydrocarbon the spectrum exhibits poorly resolved vibrational structure (maximum at 35 460 cm^{-1} (282 nm)). The fluorescence decay of 3×10^{-4} M TEA in *n*-hexane was successfully fitted to a single-exponential function for several emission wavenumbers between 29 400 and 36 400 cm^{-1} (χ^2 generally below 1.04). The fluorescence parameters obtained are compiled in Table 1 (k_F is the radiative rate and k_{NR} is the non-radiative rate, these being computed from the measured data, q_f and τ_f).

Increasing the alcohol concentration does not change the emission spectrum and the decay remains single exponential ([TEA] $< 3 \times 10^{-3}$ M), but self-quenching occurs. Both q_F and τ_F decrease according to Stern–Volmer kinetics (k_Q is the rate of self-quenching, Table 1). Self-quenching can be neglected for 3×10^{-4} M TEA.

3.3. Steady state fluorescence of the triethylamine–ethanol–n-hexane system

As ethanol is added successively to the hexane solution the emission spectrum changes its shape significanctly (Fig. 1). For $c_A < 0.02$ M, the maximum shifts approximately 800 cm^{-1} to lower energies (maximum, 34 650 cm^{-1}). The HBW increases slightly (3710 cm^{-1} in *n*-hexane to 3870 cm^{-1} for $c_A = 0.015$ M). On increasing c_A to above 0.02 M, an additional emission at lower energies arises. No extra shift of the high energy maximum is observed within the error limits. For ethanol as the quencher this new emission manifests in an increasing tail of the spectrum, extending to 20 000 cm^{-1}, but in the case of ethanol-d_1 the new emission is considerably stronger and a shoulder peaking at 27 000 cm^{-1} is observed (Fig. 1). Spectral shifts caused by addition of ethanol and deuterated ethanol are further demonstrated by the dependence of the centre of gravity of the spectrum on the alcohol concentration (Fig. 2). There is a considerable shift in $\langle \tilde{\nu}_f \rangle$ for

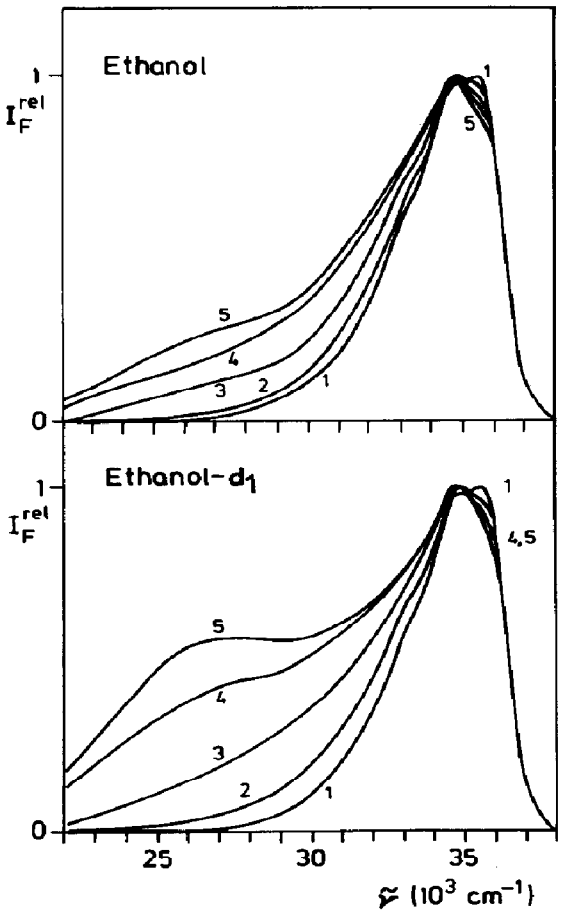

Fig. 1. Fluorescence spectra of TEA (3×10^{-4} M, $\tilde{\nu}_{exc} = 40\,800$ cm^{-1}, $T = 21$ °C) in *n*-hexane (curve 1), ethanol–*n*-hexane (formal ethanol concentrations: curve 2, 0.015 M; curve 3, 0.035 M; curve 4, 0.050 M; curve 5, 0.10 M) and ethanol-d_1–*n*-hexane (formal ethanol-d_1 concentrations: curve 2, 0.012 M; curve 3, 0.020 M; curve 4, 0.035 M; curve 5, 0.050 M) solutions.

TABLE 1

Fluorescence properties of 3×10^{-4} M triethylamine in *n*-hexane ($\tilde{\nu}_{exc} = 40\,800$ cm^{-1}; $T = 21$ °C) and rate k_q of self-quenching in the concentration range (3×10^{-4}) - (3×10^{-3}) M

q_f	0.67 ± 0.03
τ_f (ns)	28.35 ± 0.05
k_F (s^{-1})	$(2.4 \pm 0.1) \times 10^7$
k_{NR} (s^{-1})	$(1.1 \pm 0.1) \times 10^7$
k_q (M^{-1} s^{-1})	$(8 \pm 2) \times 10^8$

$c_A > 0.015$ M, concomitant with the rise of the new emission. In the case of ethanol-d_1 addition, a limiting value of $\langle\tilde{\nu}_f\rangle = 29\,900$ cm^{-1} is reached at $c_A = 0.1$ M.

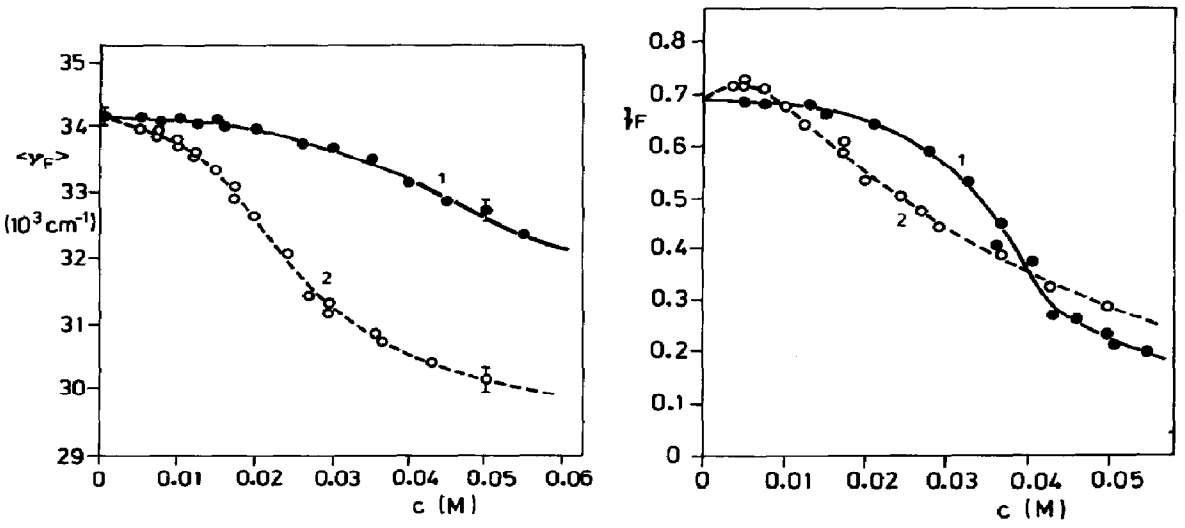

Fig. 2. Dependence of the centre of gravity $\langle\tilde{\nu}_f\rangle$ of the fluorescence spectra of 3×10^{-4} M TEA in *n*-hexane–ethanol (curve 1) and *n*-hexane–ethanol-d_1 (curve 2) mixed solvents on the formal alcohol concentration (T = 21 °C).

Fig. 3. Dependence of the absolute fluorescence quantum yield q_f of 3×10^{-4} M TEA in *n*-hexane–ethanol (curve 1) and *n*-hexane–ethanol-d_1 (curve 2) mixed solvents on the formal alcohol concentration.

The alcohol concentration dependence of the TEA absolute quantum yield q_F is plotted in Fig. 3. Fluorescence quenching, which is small for $c_A < 0.015$ M, increases considerably at higher concentrations. For addition of ethanol-d_1 the onset of the marked decrease in both q_f and $\langle\tilde{\nu}_f\rangle$ is at considerably lower concentrations ($c_A < 0.01$ M) than for the non-deuterated form. Above $c_A = 0.05$ M differences in the yields and their concentration dependence of the two alcohols are small.

The effects of temperature on the emission spectra of TEA in 0.05 M ethanol and ethanol-d_1 are presented in Fig. 4. For ethanol additions the low energy tail emission decreases gradually as the temperature rises, whilst the shoulder observed for deuterated ethanol shifts to lower energies.

The temperature dependence of the fluorescence quantum yield is plotted in Fig. 5 for TEA in pure *n*-hexane and after adding 0.05 M ethanol or ethanol-d_1 to the *n*-hexane. For both deuterated and non-deuterated ethanol q_f increases steeply above 30 °C and approaches the pure *n*-hexane value at $T > 60$ °C.

3.4. Fluorescence decay of the triethylamine–ethanol–n-hexane system

Decay functions of the TEA–ethanol and TEA–ethanol-d_1 systems in *n*-hexane were studied at various alcohol concentrations and emission wavelengths. Excitation was generally at 245 nm.

Typical examples for the decay parameters obtained at low alcohol concentrations ($c_A \approx 0.015$ M ethanol and $c_A < 0.012$ M deuterated ethanol)

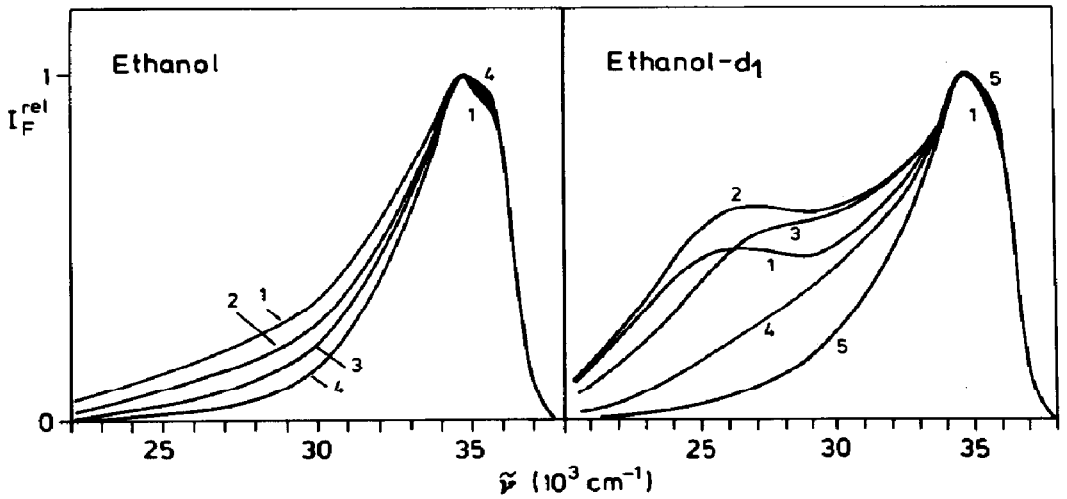

Fig. 4. Temperature dependence of TEA fluorescence spectra ($c = 3 \times 10^{-4}$ M) in *n*-hexane after addition of 0.05 M ethanol and ethanol-d_1. (Ethanol: curve 1, 13 °C; curve 2, 30.3 °C; curve 3, 41.4 °C; curve 4, 52 °C. Ethanol-d_1: curve 1, 13 °C; curve 2, 25 °C; curve 3, 35 °C; curve 4, 45 °C; curve 5, 53 °C.)

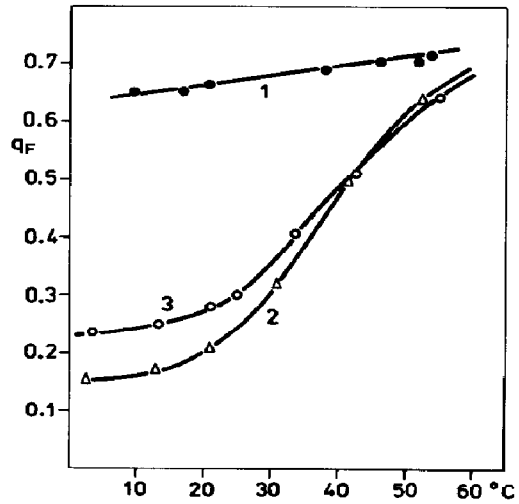

Fig. 5. Temperature dependence of the absolute fluorescence quantum yield q_f of 3×10^{-4} M TEA in *n*-hexane (curve 1), 0.05 M ethanol–*n*-hexane (curve 2) and 0.05 M ethanol-d_1–*n*-hexane (curve 3) binary mixtures.

in *n*-hexane are compiled in Table 2. The decays monitored in an intermediate emission range (around 32 000 cm^{-1}) were fitted successfully to a single-exponential function, but those measured at the high and the low energy side of the spectrum obeyed a double-exponential decay law. Two decay times were recovered at large wavenumbers but a rise time was followed by a decay when the emission was monitored in the low energy part of the spectrum. A fit to a single-exponential function was clearly not

TABLE 2

Decay parameters for 3×10^{-4} M triethylamine for the *n*-hexane–ethanol and ethanol-d_1 mixed solvent systems (c_A, concentration of ethanol; $T = 21$ °C, $\tilde{\nu}_{exc} = 40\,800$ cm^{-1}) for a fit to a sum of up to three exponentials (n, number of exponentials)

c_A (M)	$\tilde{\nu}_{em}$ (cm^{-1})	n	τ_1 (ns)	a_1	τ_2 (ns)	a_2	τ_3 (ns)	a_3	χ^2
0.0	34400	1	28.35 ± 0.05	0.091					1.02
Ethanol									
0.015	35700	1	27.03 ± 0.07	0.090					1.13
		2	27.56 ± 0.17	0.089	5.14 ± 1.32	0.0037			1.05
	32260	1	27.61 ± 0.07	0.092					1.04
	29400	1	28.30 ± 0.08	0.093					1.35
		2	27.65 ± 0.16	0.095	4.31 ± 0.65	−0.006			1.06
0.025	35700	2	25.15 ± 0.07	0.080	5.80 ± 0.41	0.010			0.99
	29400	2	25.35 ± 0.05	0.104	5.38 ± 0.19	−0.021			1.15
		3	25.08 ± 0.20	0.101	7.70 ± 0.75	−0.011	2.38 ± 0.52	−0.014	1.06
	27000	2	25.66 ± 0.05	0.130	4.96 ± 0.06	−0.076			1.34
		3	25.20 ± 0.10	0.136	6.96 ± 0.41	−0.058	2.10 ± 0.21	−0.036	1.07
Ethanol-d_1									
0.010	35700	2	29.46 ± 0.15	0.083	6.05 ± 0.52	0.021			1.05
	32260	1	29.50 ± 0.05	0.091					1.05
	29400	2	29.65 ± 0.12	0.093	5.40 ± 0.61	−0.011			1.06
0.025	35700	2	25.84 ± 0.08	0.036	7.16 ± 0.21	0.070			1.12
		3	30.68 ± 0.20	0.028	8.79 ± 0.60	0.067	2.56 ± 0.80	0.016	1.04
	28550	2	32.86 ± 0.09	0.103	4.48 ± 0.05	−0.064			1.15
		3	31.98 ± 0.33	0.106	5.66 ± 0.37	−0.053	1.70 ± 0.29	−0.023	1.05
	26300	2	31.25 ± 0.35	0.185	9.14 ± 0.30	−0.182			1.05

successful as χ^2 is large and the residuals are distributed non-randomly. The slow components decay with the same rate at all emission wavenumbers and the short times also agree to within the limits of error. The obtained concentration dependence of the decay times is plotted in Fig. 6. The full lines drawn are discussed below.

On increasing c_A to above 0.15 M the decay becomes more complex. For $c_A = 0.025$ M the experimental decay functions monitored at 36 360 cm^{-1} and 29 400 cm^{-1} are plotted in Fig. 7. Plots of the weighted residuals obtained on trying to fit the low energy decay to a sum of two or three exponential terms are also shown in Fig. 7. The parameters obtained are compiled in Table 2. For the 29 400 cm^{-1} emission two rise times and a slow decay were recovered by the reconvolution. Trying to fit the data with only one rise time gives a non-random residual plot (plot 1a in Fig. 7) at short times after the start of the pulse. The two rise times are well separated, as indicated by the low error limits and also by the correlation matrix.

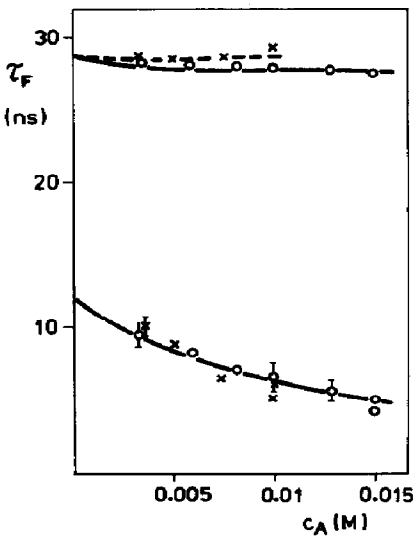

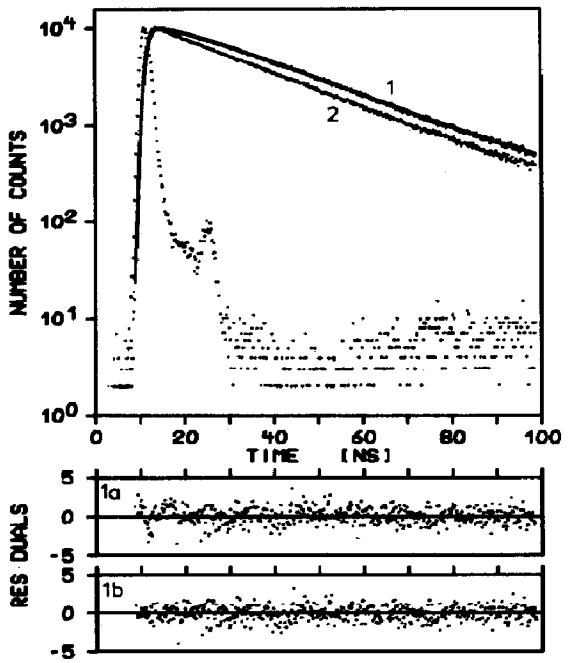

Fig. 6. Alcohol concentration dependence of the measured decay times (at $\tilde{\nu}_{em}$ = 35 700 cm^{-1} and $\tilde{\nu}_{em}$ = 29 400 cm^{-1}) for 3 × 10^{-4} M TEA in ethanol–*n*-hexane (○) and ethanol-d_1–*n*-hexane (×) mixtures in the low concentration range (T = 21 °C). The lines give the decay times calculated from eqn. (4) using the parameters given in Table 4.

Fig. 7. Fluorescence decay for 3 × 10^{-4} M TEA in 0.025 M ethanol–*n*-hexane monitored at 29 400 cm^{-1} (curve 1) and 35 700 cm^{-1} (curve 2) (T = 21 °C) and plots of the weighted residuals for a fit of the 29 400 cm^{-1} decay to a sum of two (1a) or three (1b) exponentials.

Monitoring the emission at lower wavenumbers gives essentially the same results; the grow-in and the deviation from the bi-exponential function is, however, more pronounced (Table 2).

Most importantly, at the high energy flank of the spectrum only two decay times were recovered by the fit procedure. The long decay time is in good agreement with that obtained for the low energy tail, but the short decay time does not fit to either of the two rise times. Fitting the measured decay to a sum of three exponentials either by optimizing all three decay times or by constraining one lifetime to the value of one of the rise times gave large error limits for at least one of the short decay times, making them indistinguishable. Both short decay times appear to be highly correlated in this emission range and only an intermediate time, nearer in value to the larger decay time, was recovered. This result can most reasonably be rationalized by the efficient cancellation of the fast decay and build-up in this spectral range. Therefore τ_3 contributes insignificantly.

Examination of the decay parameters obtained for TEA in (0.025 M ethanol-d_1)–n-hexane (Table 2) leads to a slightly different problem. At 26 300 cm^{-1} one rise time is followed by the decay (Table 2). At intermediate energies (29 400 cm^{-1}), however, two rise times are recovered and in the high energy part of the spectrum three decaying components are found. However, only τ_1 and τ_3 agree at all wavenumbers and the τ_2 in the low and high energy part of the spectrum are equal. τ_2 obtained at 29 400 cm^{-1} is, however, definitely different from the values obtained at the other two wavenumbers. As these intermediate lifetimes (τ_2) differ by less than a factor of 2 (5.66 ns and 9.14 ns), both appear to be artifactually correlated [26]. Correlation analysis showed that they therefore cannot be recovered independently in the analysis of the 35 700 cm^{-1} decay. For the grow-in measured at 26 300 cm^{-1} and 29 400 cm^{-1} one of these rise times predominates. The data compiled in Table 3 are typical for the corresponding spectral ranges and these alcohol concentrations.

Experimentally obtained decay functions for TEA monitored at 35 700 and 26 300 cm^{-1} in the presence of 0.05 M ethanol and ethanol-d_1 in n-hexane are plotted in Fig. 8 for T = 21 °C and T = 54 °C. The obtained time profiles show essentially a lengthening of the decay time with rising temperature, and at T = 54 °C they are nearly identical with those for TEA in pure n-hexane. At the lower temperatures different behaviour was found for the two alcohols. In the TEA–ethanol system the low and the high energy decays are parallel. However, when 0.05 M ethanol-d_1 is added, emission after 10 ns is exclusively found at lower wavenumbers.

The obtained best-fit parameters are compiled in Table 3. τ_1 increases remarkably as the temperature of the solution rises and the decays become considerably less complex. The data obtained for different emission wavenumbers agree satisfactorily with each other. Contributions of τ_3 to the 26 300 cm^{-1} emission at 21 °C are assumed to be too small to be resolved. The poor agreement of the τ_2 values at T = 54 °C probably arises from the low yields of complexation which introduce large errors.

TABLE 3

Best-fit decay parameters for 3×10^{-4} M triethylamine after addition of 0.05 M ethanol or ethanol-d_1 to *n*-hexane at various temperatures ($\tilde{\nu}_{exc} = 40\,800$ cm^{-1}; *n*, number of exponential functions)

T (°C)	$\tilde{\nu}_{em}$ (cm^{-1})	n	τ_1 (ns)	a_1	τ_2 (ns)	a_2	τ_3 (ns)	a_3	χ^2
Ethanol									
21	35700	3	9.39 ± 0.05	0.048	3.29 ± 0.36	0.015	0.95 ± 0.35	0.006	1.06
	29400	3	9.50 ± 0.57	0.075	3.37 ± 0.74	−0.018	1.38 ± 0.25	−0.021	1.05
	26300	2	9.63 ± 0.02	0.104	2.95 ± 0.03	−0.980			1.07
42	34500	2	21.91 ± 0.08	0.077	4.07 ± 0.09	0.023			1.06
	28570	3	21.99 ± 0.20	0.094	4.25 ± 0.21	−0.031	1.09 ± 0.15	−0.022	1.04
54	34500	2	26.80 ± 0.05	0.086	3.68 ± 0.69	0.008			1.06
	28570	2	26.82 ± 0.09	0.098	1.88 ± 0.07	−0.031			1.04
Ethanol-d_1									
21	34500	3	14.82 ± 0.50	0.008	5.13 ± 0.42	0.079	2.25 ± 0.50	0.040	1.05
	28570	2	14.18 ± 0.42	0.117			1.58 ± 0.20	−0.117	1.04
	26000	2	15.02 ± 0.41	0.193	4.51 ± 0.28	−0.188			1.03
43	34500	3	31.52 ± 0.21	0.047	4.52 ± 0.23	0.059	1.63 ± 0.57	0.014	0.98
	28570	3	31.35 ± 0.08	0.111	4.19 ± 0.34	−0.034	1.19 ± 0.10	−0.053	1.02
56	34500	2	28.01 ± 0.09	0.084	2.57 ± 0.09	0.027			1.01
	28570	2	27.71 ± 0.08	0.078	1.78 ± 0.05	−0.039			1.08

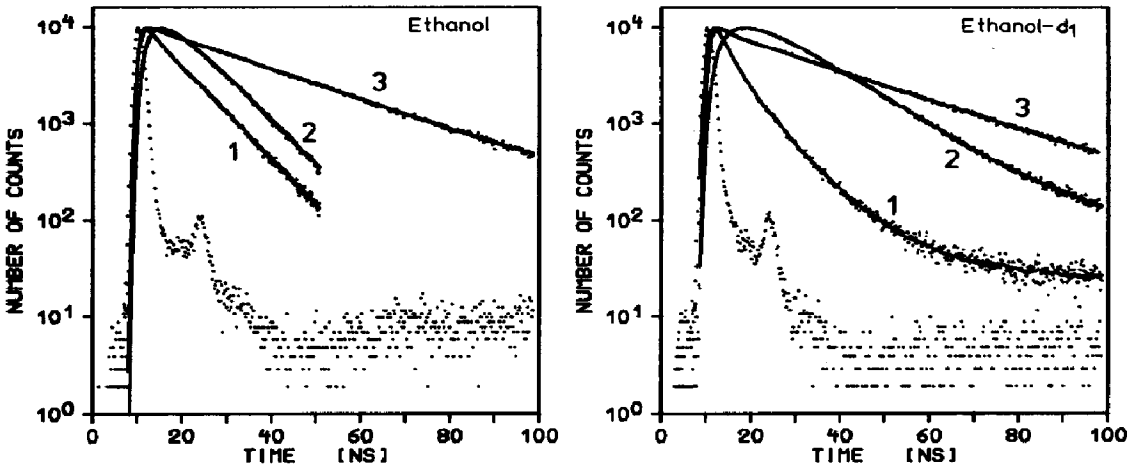

Fig. 8. Fluorescence decay functions obtained for 3×10^{-4} M TEA in 0.05 M ethanol–*n*-hexane and 0.05 M ethanol-d_1–*n*-hexane mixtures (T = 21 °C), monitored at 35 700 cm^{-1} (curve 1) and 26 300 cm^{-1} (curve 2) (in both cases T = 21 °C) and at 35 700 cm^{-1} for 53 °C (curve 3).

3.5. The triethylamine–tetrahydrofuran–n-hexane system

For comparison, emission spectra of the TEA–THF–*n*-hexane system for some low ether concentrations are shown in Fig. 9. THF concentrations below 0.2 M affect the spectra in the same way as very low alcohol concentrations and the spectra peak at the same wavenumber. Above 0.2 M THF the spectra shift gradually to lower energies. Some spectral data for this system are compiled in Table 4.

The decays were found to be fitted fairly well by a single exponential function and the decay time decreases only slightly (in 0.17 M THF and at

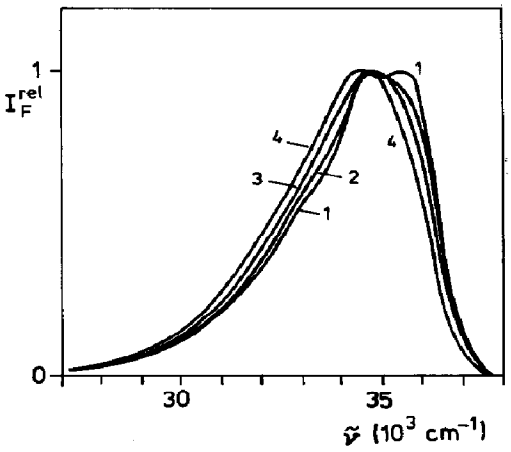

Fig. 9. Fluorescence spectra of 3×10^{-4} M TEA in *n*-hexane–THF binary mixtures at 21 °C (concentration of THF: curve 1, 0.0 M; curve 2, 0.09 M; curve 3, 0.18 M; curve 4, 0.31 M).

TABLE 4

Spectral parameters (maximum $\tilde{\nu}_{max}$, centre of gravity $\langle\tilde{\nu}_f\rangle$ and half-bandwidth HBW) for the TEA–THF system in *n*-hexane ($c_{TEA} = 3 \times 10^{-4}$ M; $\tilde{\nu}_{exc} = 40\,800$ cm^{-1}; $T = 21$ °C)

c_{THF} (M)	$\tilde{\nu}_{max}$ (×10^3 cm^{-1})	$\langle\tilde{\nu}_f\rangle$ (×10^3 cm^{-1})	HBW
0.0	35.46	34.10	3.70
0.09	34.80	34.04	3.71
0.18	34.80	33.90	3.80
0.31	34.60	33.70	3.94

$T = 21$ °C, $\tau_f = 26.9 \pm 0.1$ ns). There was, however, some indication of a second, concentration dependent, component, but its contribution was too small to be clearly resolved.

4. Discussion

The shape of the fluorescence spectra of TEA in *n*-hexane changes significantly after addition of small amounts of ethanol (Fig. 1). As long range electrostatic interactions can be neglected at these alcohol concentrations, this suggests that this is an example of the formation of fluorescing exciplexes between aliphatic tertiary amines and saturated alcohols.

In order to obtain information on the character of the amine excited state, it is worthwhile to compare the photophysical parameters and spectra of TEA in the vapour phase with those of TEA in pure hydrocarbon solvents. The condensed phase spectra coincide with the vapour spectra [27] and are only slightly red shifted. q_f and τ_f decrease in solution with respect to the vapour phase [27]. However, non-radiative processes are primarily induced by solute–solvent interactions. The radiative rate increases slightly ($k_F = 1.71 \times 10^7$ s^{-1} for isolated TEA [27]) and this can largely be attributed to refractive index effects in the condensed phase (using $n = 1.375$ for *n*-hexane and assuming proportionality to n^2 [28], one obtains $k_F = 3.2 \times 10^7$ s^{-1}).

The observed conformity of TEA excited state data in the vapour and condensed phases proves the validity of earlier suggestions that the excited orbitals remain essentially Rydberg-like on changing the phase [10]. This is also supported by *ab initio* model calculations on intermolecular perturbation of Rydberg excited states [29, 30].

The changes in the shape of the TEA fluorescence spectrum on alcohol addition are strongly dependent on the ethanol concentration (Fig. 1). At very low concentrations ($c_A < 0.02$ M for ethanol and $c_A < 0.015$ M for ethanol-d_1) good evidence for the appearance of 1:1 TEA–ethanol complexes was found. This stems essentially from (a) the significant changes in

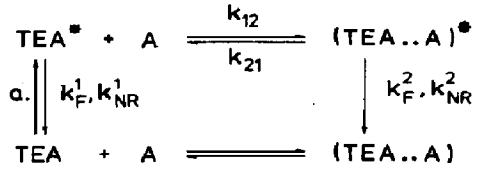

Fig. 10. Kinetic scheme for primary exciplex formation.

the shape of the spectrum and the 800 cm^{-1} red shift of the maximum and (b) that the decay kinetics expected from Fig. 10 are obeyed.

Exciplex kinetics have recently been discussed in detail [23, 31]. The mechanism of Fig. 10 leads to the following expressions for monomer (M) and exciplex (E) decay [23, 31]:

$$i_M(t) = a_1 \exp\left(-\frac{t}{\tau_1}\right) + a_2 \exp\left(-\frac{t}{\tau_2}\right)$$
$$i_E(t) = a_3 \exp\left(-\frac{t}{\tau_1}\right) + a_4 \exp\left(-\frac{t}{\tau_2}\right) \quad (2)$$

and since the initial exciplex concentration is zero, the following relation holds:

$$a_3 = -a_4 \quad (3)$$

A sum of two exponentials should thus fit the fluorescence decay data and the obtained decay times correspond to the exponential parameters in eqn. (1). The $\tau_{1,2}$ are given by

$$\frac{1}{\tau_{1,2}} = \frac{1}{2}\left[k_1 + k_2 \mp \{(k_1 - k_2)^2 + 4k_{12}k_{21}c_A\}^{1/2}\right] \quad (4)$$

where $k_1 = k_{10} + k_{12}c_A$ and $k_2 = k_{20} + k_{21}$ with $k_{10} = k_F^1 + k_{NR}^1$ and $k_{20} = k_F^2 + k_{NR}^2$. One of these values ($\tau_2$) can be interpreted as the inverse of the relaxation time for the attainment of a monomer–dimer equilibrium and the other as the fluorescence decay of the TEA–alcohol system in equilibrium. When monomer and exciplex emission overlap, the pre-exponential factors obtained from the reconvolution, a_1' and a_2', at a selected wavenumber $\tilde{\nu}_{em}$ are then given by a linear combination of the appropriate a_i weighted by the relative fluorescence intensities f_M and f_E at $\tilde{\nu}_{em}$.

$$a_1' = a_1 f_M(\tilde{\nu}_{em}) + a_3 f_E(\tilde{\nu}_{em})$$
$$a_2'' = a_2 f_M(\tilde{\nu}_{em}) + a_4 f_E(\tilde{\nu}_{em}) \quad (5)$$

Therefore, the coefficients obtained by the fit procedure must not satisfy eqn. (2) as the fast decay of the monomer and the increase in the dimer emission cancel each other at least in part.

The concentration dependence of the exponential terms (Fig. 7) can be described by eqn. (3). The rate constants found by a computer-aided fit of the solutions of eqn. (3) to the measured decay times ($c_A < 0.015$ M ethanol

TABLE 5

Best-fit rate parameters according to the kinetic scheme in Fig. 10 for ethanol and ethanol-d_1 ($c < 0.015$ M; $T = 21$ °C)

Rate ($\times 10^7$ s^{-1})	*Ethanol*	*Ethanol-d_1*
k_1	3.53	3.53
k_2	3.7	3.4
k_{12}	750.0	850.0
k_{21}	4.5	4.0

and $c_A < 0.01$ M ethanol-d_1) by variation of k_2, k_{12} and k_{21} (k_1 is taken as identical with $1/\tau_1$ at $c_A = 0$ M) are presented in Table 5. The lines in Fig. 7 are calculated from these best-fit values by means of eqn. (3). The results obtained for the TEA–ethanol system are in good agreement with preliminary data presented previously [15]. Thus the exciplex kinetics of Fig. 10 can explain the concentration dependence of the measured decay times in this low concentration range.

Monomer and exciplex emissions are characterized by nearly identical spectral and photophysical parameters, the spectra overlap significantly and q_f and τ_1 vary only slightly. k_{20} is smaller for ethanol-d_1 than for ethanol, and this can most reasonably be attributed to an increase in the non-radiative rate, as both q_f and τ_1 rise in the deuterated form. The association reaction is nearly diffusion controlled (about 10^{10} s^{-1}) and dissociation is comparable with the rate of the decay of the exciplex. Thus, multiple encounter and dissociation reactions characterize excited state processes. The equilibrium constant obtained from $K = k_{12}/k_{21}$ gave a binding energy of 12.5 kJ mol^{-1} for ethanol and 13.1 kJ mol^{-1} for ethanol-d_1. This difference may be explained in terms of the kinetic isotope effect [32]. The small binding energy rationalizes the small spectral shift of the exciplex emission compared with that of the monomer. Ground state repulsion must thus be small as well.

The influence of THF ($c < 0.2$ M) on the emission spectra is essentially equal to that described above for low alcohol concentrations (Fig. 9 and Table 4). Contrary to alcohols, however, no clear-cut kinetic evidence for exciplex formation was found. As the changes in the spectra occur in a concentration range one order of magnitude higher, the equilibrium constant should decrease by one order of magnitude (equivalent to a decrease in the binding energy to about 8 kJ mol^{-1}). A larger dissociation rate k_{21} should primarily result, as association is nearly diffusion controlled. The inverse of k_2 is an upper limit for τ_2, which should consequently decrease considerably. In connection with the efficient spectral overlap the low value of τ_2 makes it impossible to determine the exciplex kinetics.

There is good spectral evidence that TEA forms equivalent primary exciplexes with THF and alcohols, the complexes with the latter, however, having a larger binding energy. This could either be caused by steric effects

as the molecules approach each other or by the electrostatic interaction energies being smaller.

For $c_A > 0.015$ M ethanol and $c_A > 0.01$ M ethanol-d_1 the spectra and the kinetics change significantly. A low energy emission below about 30 000 cm^{-1} rises, the overall spectral shift increases (Fig. 2) and q_f drops. For 0.05 M ethanol-d_1 the new low energy band peaks at 26 500 cm^{-1}.

In Fig. 11 the emission spectra for two concentrations are partitioned into the primary and the low energy exciplex spectra. For this purpose an appropriate emission spectrum of the TEA–THF system was assigned to the primary exciplex/monomer band and fitted to the high energy flank of the measured spectrum ($\tilde{\nu} > 35\,000$ cm^{-1}). The THF concentration was adjusted by minimizing the sum over the squared deviations of the TEA–THF spectrum from the measured spectrum in the respective emission range where the fit was carried out.

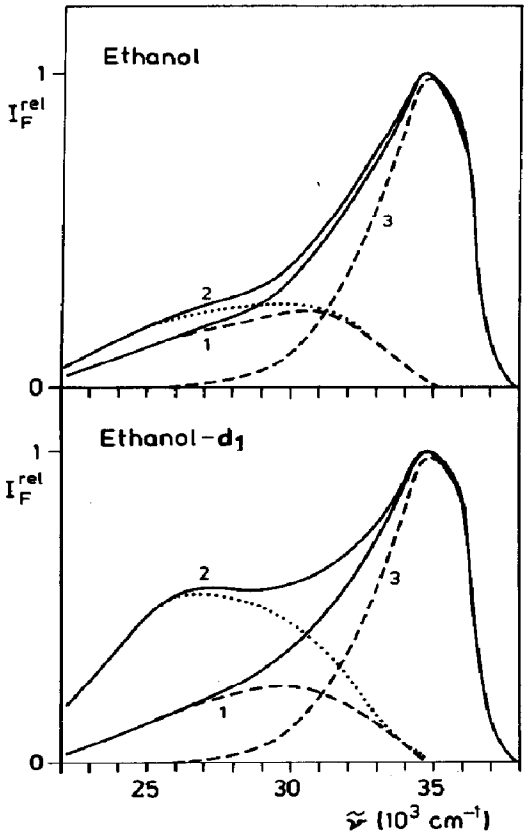

Fig. 11. Decomposition of the fluorescence spectra of 3×10^{-4} M TEA after addition of 0.05 M (curve 1) and 0.1 M (curve 2) ethanol as well as 0.03 M (curve 1) and 0.05 M (curve 2) ethanol-d_1 (T = 21 °C) according to the procedure given in the text. Curve 3 is the spectrum of the appropriate TEA–THF system for the respective higher alcohol concentration.

The peak energies (30 500 and 26 500 cm^{-1} respectively) and the shape of the difference spectra for non-deuterated and deuterated ethanol differ considerably (Fig. 11). For ethanol concentrations below 0.05 M the shape of the difference spectrum is independent of concentration. It is therefore concluded that two new emissions occur at these alcohol concentrations and in the following discussion they are referred to as I for the primary exciplex at the low concentrations and as II and III for the two emissions peaking at about 31 000 cm^{-1} and at 26 500 cm^{-1} respectively.

The TEA–ethanol-d_1 system relaxes predominantly to III and the non-deuterated form to II. This is also clearly demonstrated by the stronger decline of $\langle\tilde{\nu}_f\rangle$ above $c_A = 0.02$ M for the deuterated system in comparison with the non-deuterated system (Fig. 2).

Emissions II and III arise from exciplexes which derive from the monomer (I), as shown by the grow-in found in the appropriate emission range. Furthermore, the sum over the coefficients obtained at 26 300 cm^{-1} is nearly zero.

The decay kinetics give further evidence for the existence of two low energy exciplex emissions, II and III. For the addition of 0.025 M ethanol-d_1 three different relaxation times are recovered besides the slow decay (Table 2), indicating three different decay channels. In the TEA–ethanol system, equilibrium between the different exciplex forms is attained and the system decays with a common lifetime (parallel decay functions in Figs. 7 and 8). The equilibrium lifetime τ_1 for 0.05 M ethanol and the 35 700 cm^{-1} decay account for 97% of the intensity. For the TEA–(0.05 M ethanol-d_1) emission at 35 700 cm^{-1} this fraction is, however, only 18%, but 67% reacts to form III and the remaining 15% to form II. This shows the large isotope effect on the stability of III. The monomer-to-I reaction participates too little in the TEA–ethanol-d_1 decay to be resolved.

On raising the temperature, the low energy tail observed for 0.05 M ethanol solutions decreases gradually, but the difference spectrum does not change in shape. For the same concentrations of deuterated ethanol, however, the 30 500 cm^{-1} peak associated with III vanishes above 40 °C and the spectrum becomes almost identical in shape with that obtained for non-deuterated ethanol. This indicates the different temperature dependences of the rates of formation and dissociation of exciplex forms II and III.

The destruction of the exciplexes with increasing temperature is also indicated by the temperature dependence of q_f and τ_1. Both approach the values in the pure hydrocarbon at $T > 50$ °C. The decay kinetics becomes more simple and multi-exponential contributions decrease. It is found that III is formed only below 40 °C.

Emission from exciplex II is formed for both quenchers, ethanol and ethanol-d_1. Concomitant to the formation of II, q_f decreases for both alcohols. τ_1 decreases, however, only for ethanol, but rises when ethanol-d_1 is added. In the latter case the equilibrium lifetime passes through a maximum as the temperature increases and consequently complexes of form II are primarily observed. This is in accordance with the concentration dependence

of τ_1 (Table 2), in which a maximum lifetime for the deuterated form was also found with rising emission from II. Thus complex II is characterized by an intermediate spectral shift compared with that of the monomer (about 4500 cm^{-1}), a decrease in the fluorescence quantum yield, a slight decrease in the lifetime for non-deuterated ethanol and a slight increase in the lifetime for deuterated ethanol.

Exciplex III results almost exclusively in complexation reactions with deuterated ethanol. In this case it is the main relaxation product. Back reaction is slow and the deuterium isotope effect on the rate is responsible for the high stability of III. Back reaction in the equivalent non-deuterated form must be fast. There is, however, no clear-cut correlation between the efficiency of fluorescence quenching above $c_A = 0.025$ M and the yield of the various exciplexes. This is probably associated with the operation of a further mechanism, which is unrelated to TEA–ethanol complexation.

Information on the possible geometries of these different exciplex forms can be deduced from the *ab initio* model calculations on the excited state rearrangement processes of ammonia–water complexes published recently [16]. These calculations supported the view that intermolecular interactions in diffuse spatially extended excited states should primarily result from electrostatic attraction or repulsion between the cationic core of the excited amine and the adjacent polar solute molecule. Two main excited state relaxation pathways were discussed. The first leads to a loosely bound complex between planar ammonia and a water molecule, with the nitrogen and oxygen atoms as nearest neighbours. A binding energy of −13.0 kJ mol^{-1} was obtained for the excited ammonia–water complex. The small binding energy and spectral shifts obtained for both alcohol and ether are in good agreement with these results. Exciplex I can thus be attributed to such a structure. Furthermore, symmetric exciplexes of an excited amine with two alcohols which assume the above geometry should likewise be formed as the concentration of alcohol increases. It is reasonable to associate structure II with such an exciplex.

The second relaxation pathway found in the model calculations involves hydrogen atom transfer from water to ammonia and leads to a structure which can best be characterized as an associate between an ammonium radical ($NH_4^{\cdot}$) and a hydroxyl radical. On the excited state surface this reaction could probably originate out of structure I by motion of the alcohol hydrogen atom towards the nitrogen, proceeding with a low rate. The large deuterium isotope effect and spectral shifts observed for III may support its assignment to such a structure.

Finally, it should be mentioned that for $c_A > 0.02$ M, cyclic alcohol associates become important in low concentration solutions of alcohols in hydrocarbons [33]. These entities could give rise to both fluorescence quenching and complexation. A detailed discussion on the mechanisms of the TEA–alcohol complexation on the basis of various kinetic models is currently in preparation.

Acknowledgments

I gratefully acknowledge the continued help from Professor N. Getoff. Financial support of the work by the Austrian Science and Research Fund (Project No. P4253) and by the Jubiläumsfonds der österreichischen Nationalbank (Project No. 2447) is gratefully appreciated.

References

1 J. B. Birks, *Photophysics of Aromatic Molecules*, Wiley-Interscience, London, 1970, p. 403.
2 H. Beens and A. Weller, in J. B. Birks (ed.), *Organic Molecular Photophysics*, Vol. II, Wiley, London, 1975, 159.
3 C. G. Freeman, M. J. McEwan, R. F. C. Claridge and L. F. Phillips, *Chem. Phys. Lett.*, *8* (1971) 77.
4 A. Halpern, *Chem. Phys. Lett.*, *6* (1970) 296.
5 Y. Muto, Y. Nakato and H. Tsubomura, *Chem. Phys. Lett.*, *9* (1971) 597.
6 H. Knibbe, D. Rehm and A. Weller, *Ber. Bunsenges. Phys. Chem.*, *72* (1968) 257.
7 M. B. Robin, *Higher Excited States of Polyatomic Molecules*, Academic Press, Vol. I, New York, 1974, p. 208.
8 P. Avouris and A. R. Rossi, *J. Phys. Chem.*, *85* (1981) 2340.
9 M. van der Auweraer, F. C. DeSchryver, A. Gilbert and S. Wilson, *Bull. Soc. Chim. Belg.*, *88* (1979) 221.
10 A. Halpern, *J. Phys. Chem.*, *85* (1981) 1682.
11 A. Halpern and K. Wryzykowska, *J. Photochem.*, *15* (1981) 147.
12 A. Halpern, *J. Am. Chem. Soc.*, *96* (1974) 4392.
13 A. Halpern, P. Ravinet and R. J. Sternfels, *J. Am. Chem. Soc.*, *99* (1977) 169.
14 A. Halpern and D. K. Wong, *Chem. Phys. Lett.*, *37* (1976) 416.
15 G. Köhler, *Chem. Phys. Lett.*, *126* (1986) 260.
16 G. Köhler and R. Janoschek, submitted for publication.
17 G. Köhler and N. Getoff, *J. Chem. Soc., Faraday Trans. I*, *76* (1980) 1576.
18 G. Köhler and N. Getoff, *J. Lumin.*, *24/25* (1981) 547.
19 H. Lami, *J. Chem. Phys.*, *67* (1977) 3274.
20 J. Zechner, G. Köhler, N. Getoff, I. Tatischeff and R. Klein, *Photochem. Photobiol.*, *34* (1981) 163.
21 G. Köhler, G. Kittel and N. Getoff, *J. Photochem.*, *18* (1982) 19.
22 P. Kirkegaard, *Rep. Danish Atomic Energy Commission, Riso, Denmark*, 1970.
23 D. V. O'Connor and D. Phillips, *Time-Correlated Single Photon Counting*, Academic Press, New York, 1984.
24 D. M. Rayner, A. E. McKinnon and A. G. Szabo, *Rev. Sci. Instrum.*, *8* (1977) 1050.
25 D. P. Stevenson, *J. Am. Chem. Soc.*, *84* (1962) 2849.
26 J. R. Knudtson, J. M. Beechem and L. Brand, *Chem. Phys. Lett.*, *102* (1983) 510.
27 C. G. Cureton, K. Hara, D. V. O'Connor and D. Phillips, *Chem. Phys.*, *63* (1981) 31.
28 R. A. Lampert, S. R. Meech, J. Metcalfe, D. Phillips and A. P. Schaap, *Chem. Phys. Lett.*, *94* (1983) 137.
29 E. Kassab, J. T. Gleghorn and E. M. Evleth, *Chem. Phys. Lett.*, *70* (1980) 151.
30 G. Köhler, *J. Mol. Struct.*, *114* (1984) 191.
31 D. V. O'Connor and W. R. Ware, *J. Am. Chem. Soc.*, *98* (1976) 4708.
32 R. A. More O'Ferral, in E. Caldin and V. Gold (eds.), *Proton-Transfer Reactions*, Chapman, London, 1975, pp. 201 - 261.
33 F. Smith, *Aust. J. Chem.*, *30* (1977) 23.